


RESEARCH ARTICLE

Investigating the dentoalveolar complex in archaeological human skull specimens: Additional findings with large volume micro-CT compared to standard methods

Angela Gurr^{1,2}  | Denice Higgins³  | Maciej Henneberg^{1,2,4} |
 Jaliya Kumaratilake^{1,2} | Matthew Brook O'Donnell⁵ | Meghan McKinnon⁶ |
 Kelly A. Hall⁷ | Alan Henry Brook^{3,8}

¹Discipline of Anatomy and Pathology, School of Biomedicine, University of Adelaide, Adelaide, South Australia, Australia

²Biological Anthropology and Comparative Anatomy Research Unit, School of Biomedicine, University of Adelaide, Adelaide, South Australia, Australia

³School of Dentistry, University of Adelaide, Adelaide, South Australia, Australia

⁴Institute of Evolutionary Medicine, University of Zurich, Zurich, Switzerland

⁵Communication Neuroscience Laboratory, Annenberg School for Communication, University of Pennsylvania, Philadelphia, Pennsylvania, USA

⁶Department of Anatomical Pathology, Laboratory Services, Royal Children's Hospital, Melbourne, Victoria, Australia

⁷School of Public Health, The University of Adelaide, Adelaide, South Australia, Australia

⁸Institute of Dentistry, Queen Mary, University of London, London, UK

Correspondence

Angela Gurr, Discipline of Anatomy and Pathology, School of Biomedicine, University of Adelaide, Adelaide, South Australia, Australia.

Email: angela.gurr@adelaide.edu.au

Funding information

Adelaide Dental School, University of Adelaide

Abstract

Archaeological investigation of the dentoalveolar complex in situ within a human skull requires detailed measurements using non-invasive techniques. Standard macroscopic and radiographic methods have limitations but large volume micro-computed tomography (LV micro-CT) scanning has the potential to acquire data at high resolution in microns. In this study, archaeological specimens are analyzed using three-dimensional data visualization software from LV micro-CT scans with the aims of (1) determining whether LV micro-CT can act as a single technique to provide detailed analysis of the dentoalveolar complex and (2) how findings from the LV micro-CT technique compare with standard methods. These aims are explored by measuring a range of human skull specimens from a rare archaeological sample requiring non-invasive methods, for multiple dental and alveolar bone health categories. The LV micro-CT technique was the *only* method to provide a full range of detailed measurements across all categories studied. A combination of macroscopic and radiographic techniques covered a number of categories, but the use of multiple methods was more time consuming, did not provide the same level of accuracy, and did not include all measurements. There were high levels of reproducibility for intra-operator scoring and good inter-operator agreement from four operators with one operator whose results were outliers. As a further investigation of the potential of the LV micro-CT technique, an additional individual, a fragile, fragmented skull of an infant was studied. This investigation confirms the value of LV micro-CT scanning as a non-invasive, accurate, single technique for the extensive analysis of the dentoalveolar complex within archaeological skulls, which also allows the relationship of different tissues to be studied in situ.

KEYWORDS

Bioarchaeology, Dentoalveolar Complex, Micro-computed Tomography, Paleo-imaging, Paleopathology

This is an open access article under the terms of the [Creative Commons Attribution-NonCommercial-NoDerivs](https://creativecommons.org/licenses/by-nc-nd/4.0/) License, which permits use and distribution in any medium, provided the original work is properly cited, the use is non-commercial and no modifications or adaptations are made.

© 2023 The Authors. *International Journal of Osteoarchaeology* published by John Wiley & Sons Ltd.

1 | INTRODUCTION

Archaeological investigation of the dentoalveolar complex in human skull samples requires detailed measurements and analysis using non-invasive techniques. Standard methods commonly used for the analysis of dentitions, which remain in situ in the alveolar bone of human archaeological skulls, include visual macroscopic and radiographic examinations. These methods have limitations. Macroscopic examinations can only provide data for the external surfaces of the teeth and jaws, whereas dental radiographs can provide data for both the external and internal structures, but the images provided are only a two-dimensional (2D) slice of the specimen and the resolution is limited. Histological analysis can provide detailed information on the internal structures of a tooth and the bone, but this method is destructive and cannot examine the structures of the dentoalveolar complex as a whole. For many archaeological samples destructive analysis is not an option.

The “large volume” micro-computed tomography (LV micro-CT) scanner has the potential to provide high-resolution datasets of all structures scanned and can accommodate larger specimens such as a human skull. Other types of CT scanners such as the cone-beam CT (CBCT) scanner (Anderson et al., 2014; Lozano et al., 2022) and/or medical CT scanner (Anderson et al., 2014; Smilg, 2017) could also accommodate such samples and have been used in many investigations. However, an important distinction between the LV micro-CT scanner and these CT systems is the thickness of the scan slices. The CBCT and the medical CT scanners produce scan slices measured in millimeters (mm) (Minnema et al., 2018; Pour et al., 2016), whereas the LV micro-CT scanners have a slice thickness in microns (μm) (Orhan, 2020; Orhan & Büyüksungur, 2019). The difference in scan slice thickness is important when investigating small changes in structures, for example, details of a dental defect could be overlooked when analysing images of scan slices which are in millimeters rather than in microns.

The LV micro-CT scanning system also produces an isotropic volumetric data set (Litzlbauer et al., 2006; Orhan, 2020; Orhan & Büyüksungur, 2019). This means that the voxels in the data set have the same resolution on all three planes, like a cube (i.e., $X = \text{width}$, $Y = \text{height}$, $Z = \text{depth/slice thickness}$). The three-dimensional (3D) images produced from a reconstructed LV micro-CT scan data set could be viewed in any orientation, and the quality of the image remains the same. Medical CT scanners use a different resolution (voxel size) on the Z plane (slice thickness) than for the X and Y planes (Minnema et al., 2018, p 133 – Table 1). The difference in the voxel size for the Z plane decreases the quality of the image when viewed in the X-Z or Y-Z planes and affects the accuracy of data collection and analysis.

The LV micro-CT scanning system has been used in research for oral surgery (Beetge et al., 2018; Stan et al., 2019; Theye et al., 2018), biomedical (Grace et al., 2022; Kusins et al., 2019; Wearne et al., 2022) and medical research (Hutchinson et al., 2016; Kramer et al., 2019; Main et al., 2021; Smit et al., 2020; Tan et al., 2022; Welsh et al., 2020), paleontology (Clement et al., 2021), and forensic investigations (Alsop et al., 2022, Braun et al., 2022, Nikolova et al., 2019, Rutty et al., 2012). The non-invasive nature of this type of micro-CT scanner, as well as its technical capabilities, suggests that it could be of great value for the investigation of rare, delicate, and valuable archaeological human remains.

Computer software used with LV micro-CT scan data sets is capable of producing high-resolution 3D images of a specimen. The information gained from detailed measurements and analysis of such images could increase the understanding of the impact of dental and oral health on the general health of an individual as well as provide data on the prevalence of craniofacial conditions in past populations. For example, there is evidence that in cases of hypodontia not only are the formed teeth and the dental arches affected but also the craniofacial complex (Kerekes-Mathe et al., 2015; Patel et al., 2018).

TABLE 1 The five individuals selected from St Mary's cemetery archaeological sample to be large volume (LV) micro-CT scanned, with age range, sex, and the number of teeth and tooth type in situ within the dentoalveolar complexes.

St Mary's ID	Dental age range (years) ^a London Atlas (AlQahtani et al., 2010)	Skeletal assessment age range (years) (Anson, 2004)	Sex	Total number of teeth in-situ in the skull	Type of dentition: permanent or primary	Maxilla/right tooth types with FDI number	Maxilla/left tooth types with FDI number	Mandible/left tooth types with FDI number	Mandible/right tooth types with FDI number
SMB 82	1–1.5 (± 3 months)	0–2	U	8	Primary	51, 52	61, 62	71, 74	81, 84
SMB 04A	3.5–4.5 (± 3 months)	2–4	U	19	Primary	51, 52, 53, 54, 55	61, 62, 63, 64	71, 72, 73, 74, 75	81, 82, 83, 84, 85
SMB 52B	11–12 (± 1 year)	8–12	U	26	Permanent and primary	11, 12, 13, 14, 15, 16, 17	21, 23, 24, 25, 26, 27	31, 32, 33, 34, 75, 36, 37	41, 42, 43, 44, 85, 46, 47
SMB 66B	Over 23.5	30–39	F	17	Permanent	12, 14, 15, 17	21, 22, 23, 27	31, 32, 33, 34	41, 42, 43, 44, 45
SMB 73	Over 23.5	30–39	M	19	Permanent	11, 12, 13, 16	21, 22, 23, 24, 28	31, 32, 33, 34, 35	41, 42, 43, 44, 45
Total number of teeth LV micro-CT scanned				89					

Sex: U = undetermined sex, F = female, M = male. Cent. = central; Lat. = lateral.

^aThe London Atlas of Human Tooth Development and Eruption.

The teeth and dental arches are complex adaptive systems (Brook, 2009; Brook et al., 2014; Brook et al., 2016), and for both fundamental studies and clinical applications, systemic interactions during development and mature functioning are important (Brook and Brook & O'Donnell, 2022). Therefore, the dentoalveolar complex needs to be studied as a whole. In previous studies, only specific individual components have been investigated for clinical purposes (Appleby et al., 2015; Beetge et al., 2017; Stan et al., 2019). The structures of the dentoalveolar complex arise from complex interactions between the tissues during development. Therefore, it is important and beneficial to study 3D digital images compared with 2D images so that all the structures and tissues of the dentoalveolar complex, in their relationship to one another, can be analysed in detail for normal and pathological changes because of development and disease.

Macroscopic and/or plain radiographic methods have been the standard techniques used in many investigations for the analysis of dentitions and their associated alveolar bone tissues, and/or the analysis of human skulls from an archaeological context (Brook & Smith, 2006; D'Ortenzio, Kahlon, et al., 2018; Heuck Henriksson et al., 2019; Manzi et al., 1999; Willmann et al., 2018). Archaeological investigations that have used an LV micro-CT scanner (Fraberger et al., 2021; Lacy et al., 2012; Trinkaus et al., 2021) did not focus on the in situ dentitions or the dentoalveolar complex.

This study aims to investigate (1) whether LV micro-CT can act as a single technique to provide a detailed analysis of these structures and (2) how findings from the LV micro-CT technique compare with standard methods. These aims will be explored by measuring a range of delicate human skull specimens from a rare archaeological sample, for multiple dental and alveolar bone health categories, and comparing these findings to standard methods. As a further test of the LV micro-CT technique, a sixth individual was scanned; the fragile, fragmented skull of an infant was chosen to investigate the potential of this method to provide data that cannot be obtained using standard methods.

2 | MATERIALS AND METHODS

2.1 | Materials – The archaeological sample

There is a scarcity of skeletal collections available for research in Australia. The recentness of colonial-era burials and a lack of necessity to move or re-use burial sites means very few 19th-century European settler cemeteries have been excavated. This makes the St Mary's Anglican Church Cemetery sample a rarity. The individuals in this sample were interred between 1847 and 1927, in an area of the cemetery that had been set aside for burials paid for by the South Australian Government. These burials were not marked with gravestone memorials and were located at the rear of the church building. Further background information, historical context, and findings from the macroscopic skeletal analysis of the St Mary's sample have been published (Anson, 2004; Gurr, Brook, et al., 2022; Gurr, Kumaratilake, et al., 2022), including the methods used for the estimation of age

range and determination of sex. The excavated individuals are identified with a site code and context number (e.g., St Mary's Burial/number 73 = SMB 73) (Anson, 2004).

This study is fundamental to the next stage of investigations of this rare historic South Australian sample, which is the detailed examination of the dentoalveolar complex of all 70 individuals. Therefore, to determine the optimum methods of investigation, the well-preserved skulls of five individuals (infant SMB 82, subadults SMB 4A and SMB 52B, and adults SMB 66B and SMB 73), (Table 1), with dentitions in situ in the dentoalveolar complex, were selected to (i) cover a probable range of ages and sexes in archaeological samples, (ii) cover the change in relationships with the dentoalveolar/craniofacial complex at different ages during development and their interactions and (iii) cover a range of specimen sizes (Supplementary Table S1). The range of ages, sex, and sizes of the five selected skulls is important to investigate the resolution that could be achieved using the LV micro-CT method and the differences in the density of the teeth and/or alveolar bone tissues at different stages of development.

The fragile, fragmented skull of the infant, SMB 58, estimated dental age range = 1–1.5 years (± 3 months) applying the London Atlas (AlQahtani et al., 2010), was selected to test the value of the non-invasive, high-resolution capabilities of the LV micro-CT scanning system.

2.1.1 | The archaeological sample – dentitions

Information for the five individuals, selected for the methodology comparison, including age range, sex, tooth type, and the number of teeth (total $N = 89$) which remained in situ, is presented in Table 1. The Fédération Dentaire Internationale (FDI) – World Dental Federation notation system was used in this study to accurately record and distinguish between permanent and primary teeth.

2.1.2 | The archaeological sample – ethics

St Mary's Anglican Church Parish requested the excavation of the free ground section of the cemetery as they wished to re-use the area and approved the study of the skeletal remains. Flinders University Social and Behavioural Research Ethics Committee approved the research (SBREC project number 8169). Destructive analysis was not permitted for the investigation of the sample as they are of a rare historical nature.

2.2 | Methods

2.2.1 | Comparative methods used

The LV micro-CT scanning system, macroscopic, and standard radiographs were used for the analysis of the dentoalveolar complex in situ in the selected archaeological human skulls.

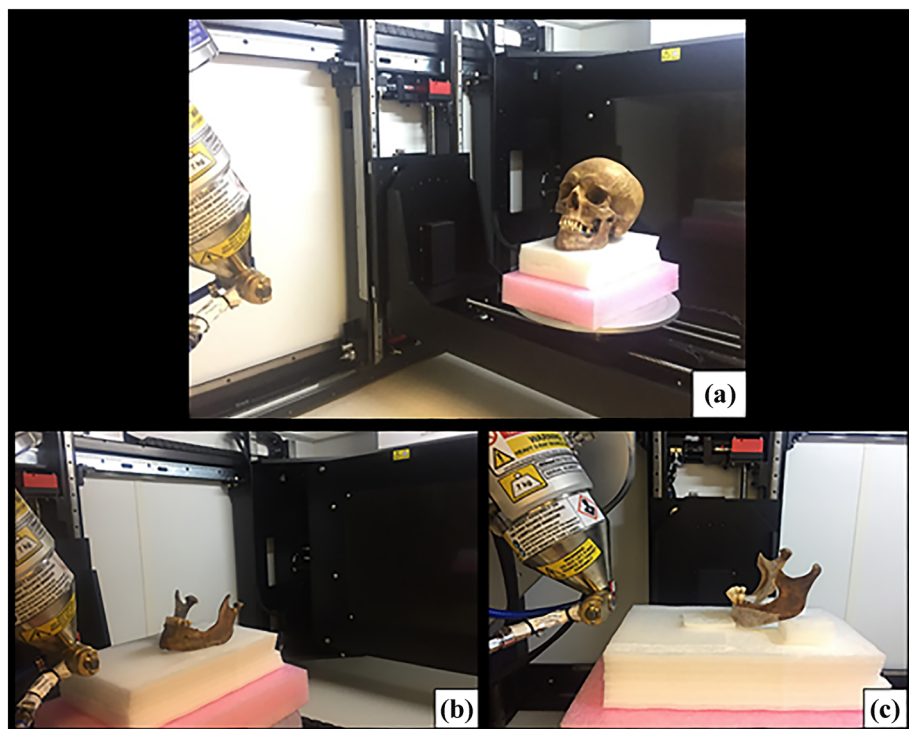


FIGURE 1 Large Volume Micro-CT. Skull SMB73 – adult male (skeletal age range 30–39 years). (a) (from left to right) X-ray source, rotation stage with the skull on polystyrene foam, (center), flat panel X-ray detector behind the skull. The skull in position before scanning using the Nikon XH T 225 ST cabinet system (Nikon Metrology, 2021). (b) Mandible only of adult SMB 73. (c) Mandible of SMB 66B – adult female (skeletal age range 30–39 years). Figure 1b, c is showing the position of the mandible with in situ dentition before scanning. © Angela Gurr. [Colour figure can be viewed at [wileyonlinelibrary.com](https://onlinelibrary.com)]

2.2.2 | Large volume micro-CT

The dentoalveolar complex was scanned using the Nikon XT H 225 ST cabinet Micro-CT scanning system (Nikon Metrology, 2021) at Flinders University (Clement et al., 2021; Wearne et al., 2022). The skull, the cranium without the mandible, and the mandible alone were scanned to investigate the achievable resolution of each specimen (Supplementary Table S2), as the spatial resolution (pixel/voxel size) selected for each scan was relative to the size of the specimen. In addition, it was important to investigate whether the positioning of the opposing maxillary and mandibular teeth within the skull, during the scanning process, could affect the analysis of the occlusal surfaces of these teeth. In choosing the scanning settings, the transmitted signal intensity and source power settings were considered according to guidelines (du Plessis et al., 2017; Wearne et al., 2022).

The skulls, of adult SMB 73 (Figure 1a) and subadult SMB 52B, were scanned at projection images 4056×4056 pixels in size, corresponding to a field of view of 243×243 mm, width \times height, at $60 \mu\text{m}$ isotropic pixel size. Full details of the parameters used (X-ray source voltage [kV], source current [μA], source power [W], filter type and thickness [mm], X-ray projections, rotation step, and exposure time in seconds) for all of the LV micro-CT scans can be found in Supplementary Table S2.

The cranium with the maxilla of adult SMB 66B, subadult SMB 4A, and infants SMB 82 and SMB 58 were scanned *without* the mandible present. These scans were performed with the same X-ray source settings and rotation step as the skulls, as shown in Supplementary Table S2, but at $50 \mu\text{m}/\text{pixel}$ (for adult SMB 66B), $55 \mu\text{m}/\text{pixel}$ (subadult SMB 4A), $40 \mu\text{m}/\text{pixel}$ (infant SMB 82), and $35 \mu\text{m}/\text{pixel}$ (infant SMB 58), corresponding to a field of view of 202×202 ,

223×223 , 162×162 , and 142×142 mm, respectively, adapting (minimizing) the pixel size according to the specimen size. The total acquisition time was 1 hour and 10 minutes per scan.

The mandible (Figure 1b, c), of the six individuals, was scanned separately from the associated cranium. For further details of the scan parameters, see Supplementary Table S2. Projection images were 4056×4056 pixels in size, corresponding to a field of view of 81×81 mm at $20 \mu\text{m}/\text{pixel}$ (for SMB 4A), 89×89 mm at $22 \mu\text{m}/\text{pixel}$ (SMB 52B), 53×53 mm at $13 \mu\text{m}/\text{pixel}$ (SMB 73 and SMB 66B), 73×73 mm at $18 \mu\text{m}/\text{pixel}$ (for SMB 82), or 85×85 mm at $21 \mu\text{m}/\text{pixel}$ (for SMB 58; source current $95 \mu\text{A}$, [18 W]). The total acquisition time was 1 hour and 40 minutes per scan. The mandible, being smaller than the entire skull or the cranium, allows higher-resolution scanning.

2.2.3 | LV micro-CT – post processing computer software

Axial cross-section images were reconstructed using CTPro3D software (Nikon Metrology, 2021) and saved as 8-bit bitmap images (256 gray levels, 0 = air, 255 = enamel). Avizo 9 (ThermoFisher Scientific, 2019) data visualization software was used for image analysis of the reconstructed scan data sets. The size of a high-resolution micro-CT scan requires a computer that has the capacity to process and navigate the reconstructed 3D volumetric data sets. Hardware constraints can sometimes require the micro-CT scan data sets to be reduced in size by one half (reading every second slice of the scan) or by one quarter (reading every fourth slice of the scan). For example, the original LV micro-CT scan data set size for the adult human skull

of SMB 73 was 33 GB at 60 $\mu\text{m}/\text{pixel}$, and this could be reduced to 533 MB at 240 $\mu\text{m}/\text{pixel}$. The scan data set for the mandible of SMB 73 was originally 42.7 GB at 13 $\mu\text{m}/\text{pixel}$ but could be reduced to 658 MB at 52 $\mu\text{m}/\text{pixel}$. The ability to change the size of the micro-CT scan data sets offers many benefits including the option to conduct an initial analysis, similar to triaging to identify the presence of pathology using the quarter or half sized scan data sets and then use the full-sized scan data sets for a more in-depth examination. To increase loading and analysis speed for this investigation, the scan data sets were reduced in size (Perilli et al., 2012).

2.2.4 | Standard methods

Macroscopic examination

Visual examination of the in situ dentoalveolar complex was conducted in a dry laboratory with the aid of a table magnification glass and enhanced lighting.

Standard radiographic methods

Intraoral periapical and bitewing radiographs were taken using Planmeca X-ray equipment (Planmeca, 2022), with Phosphor Storage Plates (PSP) as the detectors. Exposure settings were as follows: Tube voltage: 70 kV; Tube current: 6 mA, with an exposure time of 0.32 s. Extraoral radiographs of the dentoalveolar complex of each individual's skull were taken, using orthopantomogram (OPG) X-ray equipment to rotate around the maxilla and mandibular area. The X-ray source used was a Kavov Pan eXam Plus (KaVo Dental GmbH, nd). The tube type for this equipment was stationary anode; 65 kV; Tube current: 15 mA, with an exposure time of up to 16.4 s.

2.2.5 | Scoring systems and identification criteria

The dentoalveolar complexes were analysed for the following dental and alveolar bone health categories: (i) dental inventory, (ii) category of tooth wear, (iii) evidence of dental trauma, (iv) class of occlusion, (v) presence of caries, including the category of radiolucency, (vi) grade of alveolar bone status, (vii) evidence of periodontal disease (i.e., measurement of horizontal bone loss), (viii) presence of enamel hypoplastic (EH) defects, (ix) presence of areas of interglobular dentine (IGD), and (x) an estimation of dental age range (Table 2).

Enamel opacities were not recorded as enamel hypomineralization defects are difficult to distinguish from areas of staining on the tooth caused by the post-mortem environment and/or taphonomic alterations which could cause variations in the mineralization density of the dental enamel (Efremov, 1940; Garot et al., 2017; Garot et al., 2019). The criteria used for the identification and scoring of the above dental and alveolar tissue health categories are presented in Table 2.

Crania and mandibles were radiographed separately. For that reason, information about occlusion is not available from radiographs and only severe cases of EH defects (EH) and/or IGD can be identified on

radiographs; therefore, these categories were not assessed using this modality.

The bone density level of the teeth, the skull/cranium, and of the mandible of each individual was determined by applying a threshold level to the reconstructed scan data sets using the Avizo 9 software (ThermoFisher Scientific, 2019). This digital information was stored as an Avizo "project" (Figure 2a1, a2). These projects were used for the scoring of the oral health categories, using the post-processing software, as they provide a consistent and reliable platform for repeated measurements. Digitally reconstructed radiographs (DRR) (Figure 2b1, b2), together with the "clipping" tool, were used to remove a quadrant of the jaw (Figure 2c1, c2), in order to examine all the surfaces of the dentition during 3D image analysis.

2.2.6 | Validity of the scoring system of dental and alveolar bone tissue health categories

Five operators, either academic staff or postgraduate students in Biological Anthropology and/or Archaeology, were trained and calibrated before they scored the dental and alveolar bone tissue health categories independently 2 weeks after the training session (Table 2). The principal operator (AG) scored the categories for the in situ dentitions, alveolar bone tissues, and individual loose teeth not in the jaw, macroscopically, on dental radiographs, and on the 2D and 3D images produced by the Avizo software from the reconstructed scan data sets. Data scoring sessions were repeated for intra-operator reliability 2 weeks apart. Inter-operator scoring of the same categories using the same methods (Table 2) was undertaken by MM, on different dates and times from intra-operator (AG). Other operators conducted data scoring sessions for the categories (Table 2), on images produced by the LV micro-CT scan data sets only.

2.3 | Statistical analysis

Intra-operator and inter-operator reliability were assessed using Gwet's Agreement Coefficient (AC1), weighted Gwet's Agreement Coefficient (AC2), and Intraclass Correlation Coefficient (ICC) using a two-way random-effects model for absolute agreement, for binary and nominal scale data, ordinal scale data, and continuous data, respectively. All analyses were performed using Stata v17 (StataCorp, 2022).

3 | RESULTS

3.1 | Reproducibility – standard statistical analysis

Supplementary Table S3 presents a summary of the results from tests of intra- and inter-operator reliability for each of the methods assessed, followed by a brief written summary. Additional information relating to this statistical analysis can be found in the supporting information as Supplementary Table S4 and the raw data as Data_S1.

TABLE 2 Dental and alveolar bone categories, measured for the investigation of dentition and alveolar tissues in situ in the dentoalveolar complex of archaeological human skull specimens, with the identification criteria, the methods used, and the scoring systems followed for collection of data, including sources.

Categories measured	Identification criteria	Method/s to be used	System/s to be followed	Sources/references
Inventory – total number of teeth in situ	Inventory of teeth present	Macroscopic, Radiographic, LV Micro-CT	FDI (ISO 3950) notation system used, data was recorded on a visual chart representing the upper and lower permanent/primary dentition.	FDI World Dental Federation, 2022, International Organisation for Standardization, American National Standard, American Dental Association, 2010
Inventory - ante-mortem tooth loss	Evidence of healing of alveolar processes	Macroscopic, Radiographic, LV Micro-CT	Location of healed alveoli where tooth was previously located-recorded on (FDI) visual chart as above	Araújo et al., 2015, Kinaston et al., 2019
Inventory – Post-mortem tooth loss	No evidence of healing of the alveolar bone – open socket observed	Macroscopic, Radiographic, LV Micro-CT	Location of open socket in alveolar process/missing tooth type-(FDI) visual chart used as above.	Hillson, 1996
Occlusion	Position of jaws and dental arches – in relation to each other mesio-distally.	Macroscopic, LV Micro-CT	Scored using Angel's (1966) classes of malocclusion.	Angel, 1966: p34–44
Tooth wear (occlusal)	Evidence of loss of enamel and/or exposure of dentine on the occlusal surface	Macroscopic, LV Micro-CT	Category of tooth wear selected from Molnar's(1971) criteria chart.	Molnar, 1971
Dental trauma	Evidence of morphological damage to the tooth	Macroscopic, LV Micro-CT	An adaptation of the index by Winter and Brook (1989) was used to record trauma involving enamel only; enamel and dentine; or enamel, dentine, and pulp.	Winter & Brook, 1989
Caries	Evidence of decay – either involving the enamel surface, enamel and dentine or the enamel, dentine, and the pulp. Identification of a difference in radiolucency	Macroscopic, Radiographic, LV Micro-CT	Tooth type affected (FDI), the number, and location of carious lesions recorded. Dental probe was used for the macroscopic examination. ICDAS/ICCMS categories of radiolucency were selected from a visual chart for radiographic and digitally reconstructed radiographs (DDR) on Avizo 9 software.	Pitts & Ekstrand, 2013; International Caries Classification management System, 2022
Periodontal disease	(1) Alveolar bone status – evidence of changes in the structure of the buccal contours of the alveolar margins of the posterior teeth (2) Evidence of horizontal and/or vertical bone loss	Macroscopic, LV Micro-CT	(1) Alveolar bone status-inspection of the buccal contours of the alveolar margins of the posterior teeth. Scored as grade 1 to 4 using Ogden's (2008) system (2) Evidence of horizontal – measurement taken on the midline of the labial/buccal and lingual surfaces of the tooth, from the CEJ to the crest of the alveolar bone. A periodontal probe was used with 3-mm increments for the macroscopic examination.	(1) Ogden et al., 2007: p.283–307; Riga et al., 2021. (2) Perschbacher, 2014: p 302

TABLE 2 (Continued)

Categories measured	Identification criteria	Method/s to be used	System/s to be followed	Sources/references
Enamel hypoplastic defects	Evidence of enamel hypoplastic defect/s	Macroscopic, LV Micro-CT	Using an adaptation of the enamel defect index (EDI), the type of enamel hypoplastic defect/s, the number and location of defects were recorded. A measurement/s of the distance from hypoplastic defect/s to CEJ was taken.	Brook et al., 2001, Elcock et al., 2006
IGD (interglobular dentine)	Evidence of areas of defective mineralization in the dentine structure	LV Micro-CT	Recorded presence of IGD as yes/no	Colombo et al., 2019, Veselka et al., 2019
Dental age range estimation	Eruption rate and position of developing teeth in the alveolar	Macroscopic, Radiographic, LV Micro-CT	The London Atlas of Tooth Eruption and Development was used to identify the stage of eruption and tooth development.	AlQahtani, 2012, AlQahtani et al., 2010

Notes: FDI = Fédération Dentaire Internationale, ICCMS = International Caries Classification and Management System, CEJ = Cementum Enamel Junction, ICDAS = International Caries Detection and Assessment System.

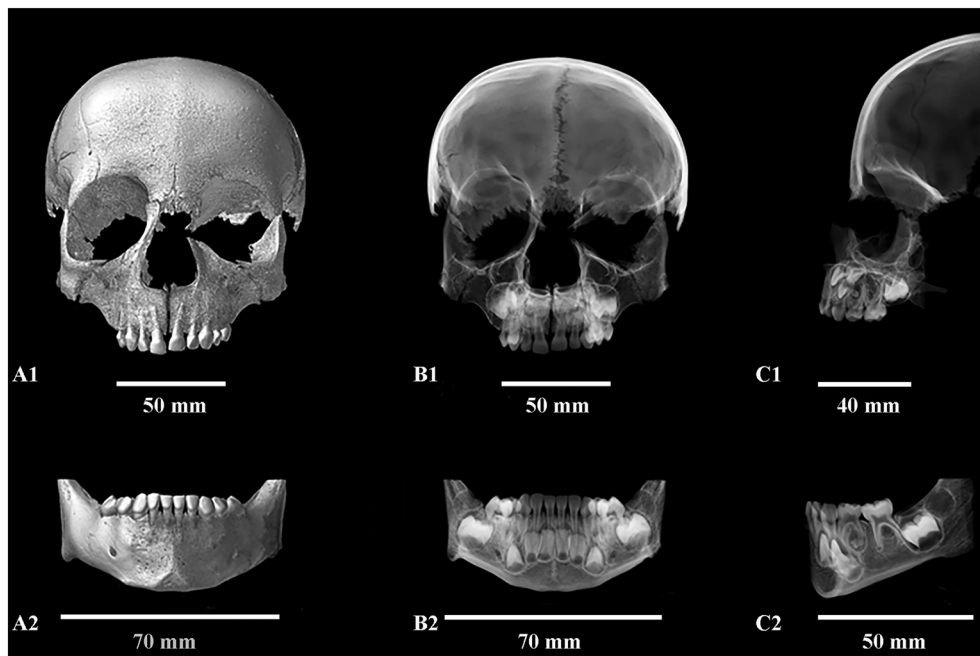


FIGURE 2 Large Volume Micro-CT. Sample SMB 4A – subadult (dental age range: 3.5 to 5.5 years; skeletal age range: 2–4 years). (cranium micro-CT scanned at 55 $\mu\text{m}/\text{pixel}$ and mandible at 20 $\mu\text{m}/\text{pixel}$). (a1, a2) Anterior/labial view of the dentition in situ in the maxilla and mandible using the Avizo 3D image function. (b1, b2) Anterior/labial view of the same dentition using the Avizo digitally reconstructed radiograph (DRR) function (ThermoFisher Scientific, 2019). (c1, c2) Lateral view of the dentition using the clipping tool to remove one side of the jaw. (b, c) The DRR is showing the developing dentition in the alveolar bones. Images were created using volren with the Avizo 9 software (ThermoFisher Scientific, 2019). © Angela Gurr.

TABLE 3 The ability of each investigative method to provide data for the analysis of the categories studied for the health of the teeth and associated alveolar bone tissues.

Was the method capable of providing data for the following categories? Y/N	Methods		
	LV micro-CT	Macroscopic	Radiographic
Inventory	Y	Y	Y
Tooth wear	Y	Y	Y
Dental trauma	Y	Y	Y
Occlusion	Y	Y	N
Caries	Y	Y	Y
Alveolar status	Y	Y	N
Periodontal disease	Y	Y	N
Enamel hypoplasia	Y	Y	N
IGD (denture defects)	Y	N	N
Dental age estimation	Y	Y	Y
Technical capabilities:			
Are internal structures visible?	Y	N	Y
Absence of superimposition problems?	Y	Y	N

Note: Y = yes; N = no. LV micro-CT = large volume micro-CT; IGD = interglobular dentine.

3.2 | Capacity for each method to provide data for the categories scored

Table 3 presents the results for each of the methods in determining the data required. The LV Micro-CT was the *only* technique to provide information for all of the categories. Macroscopic investigations could not provide data on the internal structures of the teeth (Table 3). Large volume Micro-CT and macroscopic examination were the only methods to provide information regarding the occlusion, as the maxillary and mandibular dentitions must be in their natural anatomical position (opposing each other) to score this category. The radiographic techniques did not provide data for at least 5 of the 10 investigated categories (Table 3). It was not possible to grade the alveolar bone status on the radiographs because of superimposition issues as this category examines small morphological changes in the structure of the buccal contours of the alveolar margins of the posterior teeth.

3.2.1 | Comparison of the level and range of results for the LV micro-CT, macroscopic and radiographic methods

Table 4 presents the level and range of results for each method. All three methods provided identical data for the in situ dental inventory. The estimation of the dental age range for each individual was similar when applying the London Atlas (AlQahtani, 2012; AlQahtani et al., 2010) with each method (Table 1).

Scores for the category of tooth wear for the radiographic method were consistently at least one category higher compared with the LV micro-CT and macroscopic examinations, but for dental trauma, the macroscopic technique identified the greatest number of episodes (Table 4).

The grades for alveolar bone status were scored higher for the LV micro-CT method compared with the macroscopic examination results. This category could not be scored on radiographs.

The distance from the Cemento-Enamel Junction (CEJ) on the teeth to the crest of the alveolar bone provided evidence of horizontal bone loss, an indication of periodontal disease; the measurements on the 3D images from the LV micro-CT were greater than those obtained using the macroscopic method. For example, using the LV micro-CT method, the ranges of measurements for horizontal bone loss for adult SMB 73 were 2.0 to 7.4 mm, compared with 2.0 to 6 mm using the macroscopic method.

The total number of carious lesions identified using the macroscopic method was higher than other methods (Table 4). Scoring of the category of radiolucency of carious lesions for the LV micro-CT and radiographic methods was identical (Table 4); this category could not be scored macroscopically.

More individuals were identified with evidence of EH defects by the LV micro-CT method (Figure 3), compared with the macroscopic examination (Table 4). As with the measurements for horizontal bone loss, using the LV micro-CT method the distance from the CEJ to the EH defect/s was greater than that obtained by the macroscopic examination. From the three methods compared, only the LV micro-CT technique provided data for the category of IGD.

Illustrative Case Study: Infant SMB 58, dental age range = 1–1.5 years (± 3 months) (AlQahtani et al., 2010). The accuracy of the LV micro-CT method was tested with the fragmented cranium and mandible of infant SMB 58. The standard methods were applied and EH defects were identified macroscopically on the maxillary primary canines and the semi-erupted primary maxillary and mandibular second molars of this infant. The LV micro-CT technique identified further detailed evidence of EH defects on the primary maxillary and

TABLE 4 A comparison of the levels and range of results for LV micro-CT, macroscopic, and radiographic methods of examination of the dental and alveolar bone health categories.

Categories measured	Methods used		
	LV micro-CT	Macroscopic	Radiographic
Tooth wear Molnar (1971). Grades 1 to 8. Min. to max. range observed:	1 to 5	1 to 5	2 to 5
Dental trauma Winter and Brook, (1989) Total number of teeth affected:	9	17	10
Class of occlusion Angle, (1966) Range of classes: 1 to 3	Class 1	Class 1	N/A
Cariou lesions ^a Total number of lesions observed:	56	80	41
Cariou lesions ICDAS/ICCMS Categories of radiolucency: 0 to 6 Min. to max. range observed	1 to 4	N/A	1 to 4
Enamel hypoplastic defects Brook et al. (2001) Total number of teeth affected:	44	13	N/A
IGD (interglobular dentine) Colombo et al., (2019), Veselka et al., (2019) Total number of teeth affected:	7	N/A	N/A

LV Micro-CT = large volume micro-CT. N/A = not applicable – this method cannot be used to score the specific oral health category. IGD = Interglobular dentine, ICDAS = International Caries Detection and Assessment System; ICCMS, International Caries Classification and Management System.

^aMore than one carious lesion may be present on a tooth.

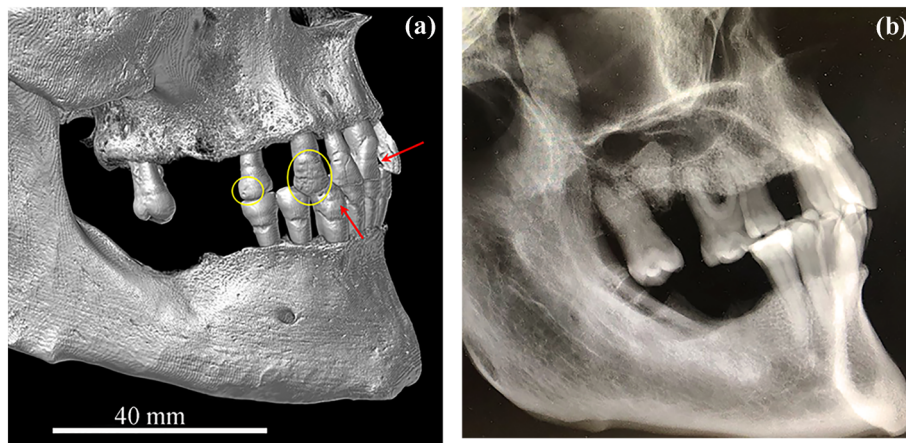


FIGURE 3 Sample SMB 73, adult male (dental age: over 23.5 years, skeletal age range: 30–39 years). (a) Large Volume Micro-CT-(skull scanned at 60 $\mu\text{m}/\text{pixel}$). Lateral view of the dentition in situ in the maxilla and mandible. Multiple examples of enamel hypoplastic (EH) defects (linear = red arrows and pits = yellow circles) are shown. The software “clipping” tool was used to remove half of the skull, therefore the upper first molar, seen on the radiograph (Figure 3b), is not visible. (b) Digitally reconstructed radiograph tool (DRR – Avizo 9 software) of the same individual. The EH defects cannot be observed on this radiograph; however, evidence of periodontal disease with generalized bone loss, most severe around the molar teeth, is visible. The bony outline of the mandible suggests that lower molars were lost because of periodontal disease. Images were created using volren with the Avizo 9 software (ThermoFisher Scientific, 2019). © Angela Gurr. [Colour figure can be viewed at wileyonlinelibrary.com]

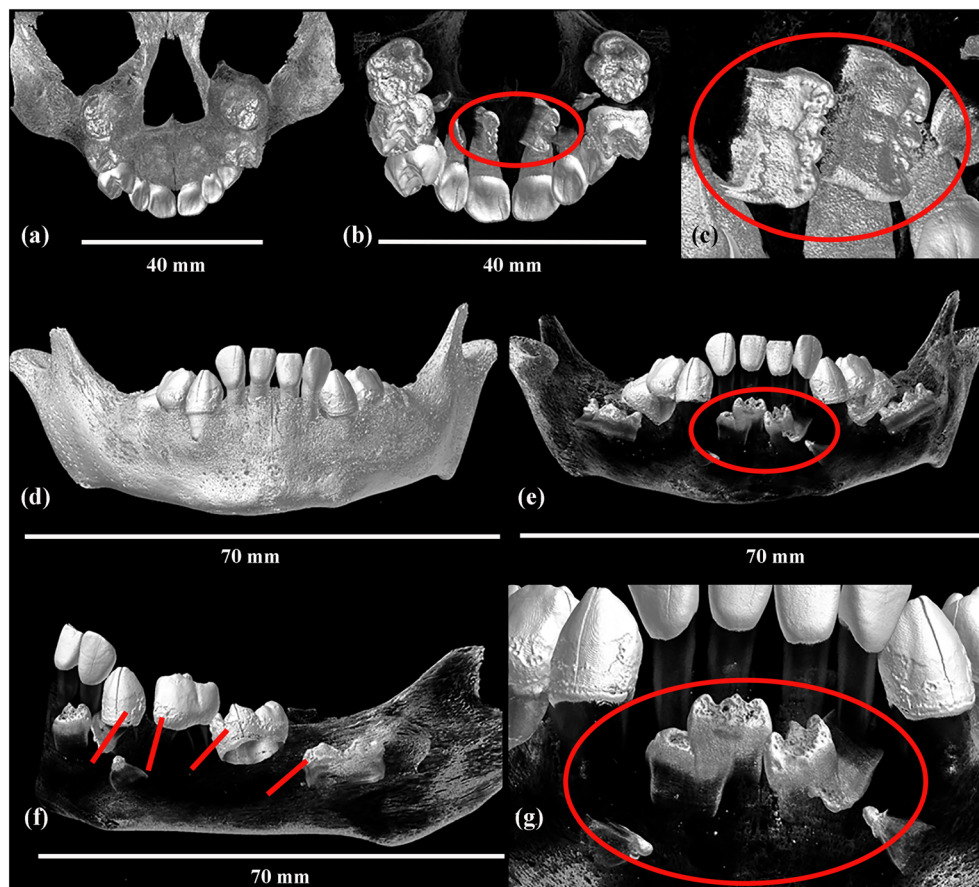


FIGURE 4 Large Volume Micro-CT. SMB 58 – Infant (dental age range 1–1.5 ± 3 months, skeletal age range 0–2 years of age). (cranium micro-CT scanned at 35 µm/pixel and mandible at 21 µm/pixel). (a and b) Posterior/lingual view of the maxilla. The bone density threshold level has been manipulated to reveal the developing teeth in the alveolar. The red oval shows the maxillary tooth germs of the permanent central incisors. Other teeth in the maxilla also have evidence of enamel hypoplastic defects. (c) Red oval – a close-up of Figure 4b, the maxillary permanent central incisor tooth germs, showing enamel hypoplastic defects. (d) Anterior/labial view of the mandible. (e–g) As with Figure 4b, the bone density threshold level was changed to show the developing teeth in the alveolar (red oval). (f) Lateral view of the mandibular dentition, the clipping tool was used to remove one side of the jaw. Red lines identify enamel hypoplastic defects on the erupted primary teeth and the semi-erupted primary second molar. Permanent teeth can be seen developing in the alveolar. (g) A close-up (from Figure 4e) of the mandibular permanent central and lateral incisor teeth developing (the red oval), and the tips of permanent canine teeth within the alveolar tissue. Images were created using the Volren function with the Avizo 9 software (ThermoFisher Scientific, 2019). © Angela Gurr. [Colour figure can be viewed at wileyonlinelibrary.com]

mandibular teeth in situ in the jaws (Figure 4), as well as on the erupting primary second molars. Extensive EH defects were also seen on the developing permanent tooth germs in the alveolar tissue (Figure 4). These enamel defects were not identified on the dental radiographs (Figure 5). Areas of IGD were identified (Figure 6) in all the teeth. These internal dentine defects (IGD) and the EH defects seen on the developing teeth within the alveolar tissue could not be identified macroscopically or radiographically (Figures 3, 5, and 6).

4 | DISCUSSION

This study demonstrated there are substantial differences between the methods, particularly in the levels and in the detail that they can be used to score each of the dental and alveolar bone health

categories. These methods are considered in the order of the aims of the study.

4.1 | Aim 1 – Can LV micro-CT act as a single technique to provide a detailed analysis of the structures of the dentoalveolar complex in situ within archaeological human skull specimens?

The high-resolution, non-invasive LV micro-CT scanning method is capable of being a single technique for the analysis of the structures of the dentoalveolar complex in situ within a human archaeological skull specimen. This technique provided data for the full range of categories measured, (Tables 2–4), fulfilling the first aim of this study. The post-scan processing software (ThermoFisher Scientific, 2019) enabled specific and detailed measurements for the external and

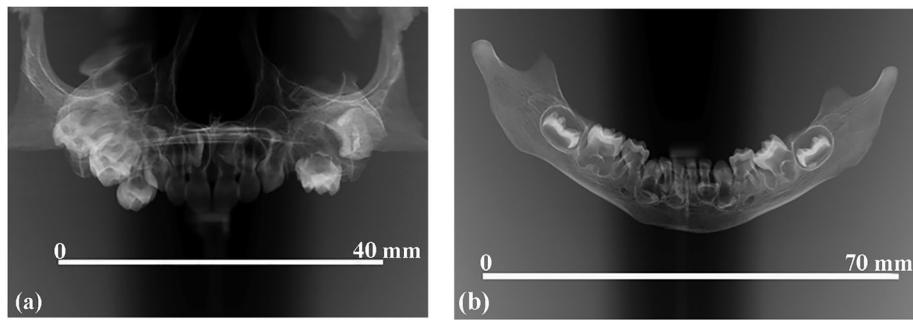


FIGURE 5 Dental radiographs. SMB 58 – Infant (dental age range $1-1.5 \pm 3$ months, skeletal age range 0–2 years of age). (a) Panoramic radiograph of the maxillary dentition, showing the erupted and semi-erupted primary teeth and the developing permanent teeth within the alveolar. (b) Panoramic radiograph of the mandibular teeth, similarly showing the erupted and semi-erupted deciduous teeth. The developing cusps of the permanent first molars can be clearly seen in the alveolar bone.

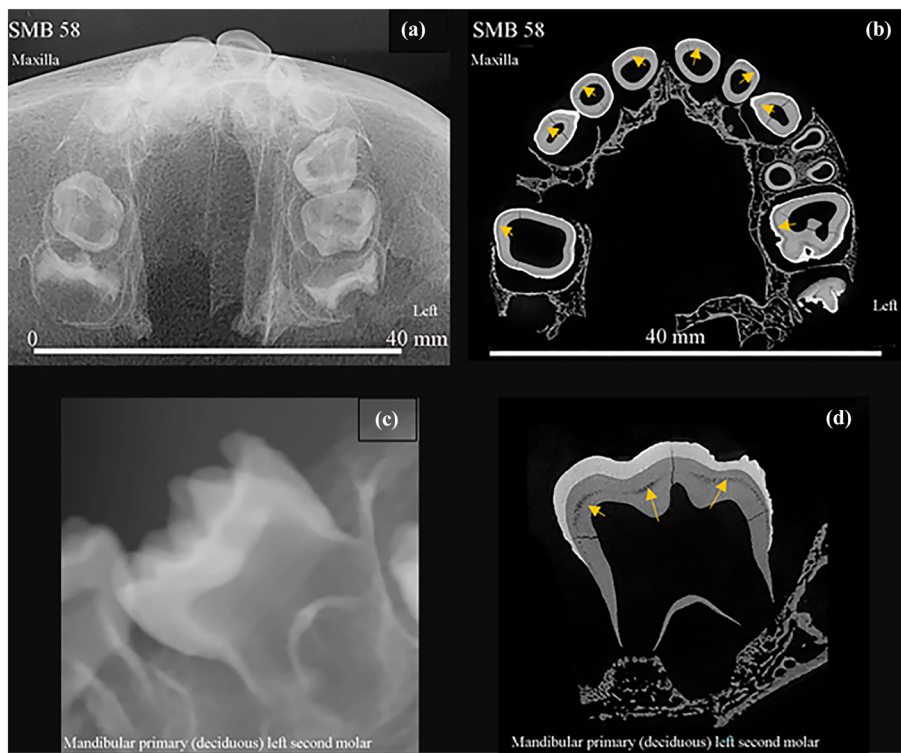


FIGURE 6 LV Micro-CT. SMB 58 – Infant (dental age range $1-1.5 \pm 3$ months, skeletal age range 0–2 years of age). (cranium micro-CT scanned at $35 \mu\text{m}/\text{pixel}$ and mandible at $21 \mu\text{m}/\text{pixel}$). (a) Dental radiograph of the maxilla (vertex occlusal projection). The level of detail visible in this dental X-ray is less when compared with the micro-CT scan slice in Figure 6b. (b) Superior view of an internal slice from the LV micro-CT scan of the maxillary teeth. Orange arrows show areas of interglobular dentine. This mineralization defect was seen in all of the maxillary teeth and the majority of the mandibular teeth. (c) A dental radiograph of the lower left primary second molar (semi-erupted). (d) Sagittal slice from the micro-CT scan of the same mandibular tooth showing interglobular dentine (orange arrows). Micro-CT images were created using the orthoslice function with the Avizo 9 software (ThermoFisher Scientific, 2019). © Angela Gurr. [Colour figure can be viewed at [wileyonlinelibrary.com](https://onlinelibrary.wiley.com/doi/10.1002/ajpa.25044)]

internal structures of the dentoalveolar complex with the ability to scroll through the 3D image. With training, the software was easy to use for operators with a non-dental background.

The analysis of the LV micro-CT scan images provided insight into the changes and interactions that occur in the teeth and alveolar bone during development and disease. These data are important as the teeth and dental arches are parts of Complex Adaptive Systems of

two or more structures (Brook, 2009, 2014; Brook et al., 2016). The age range and differing size for each individual were deliberately chosen to cover the dynamic interactions and changes that occur during development and to determine the value of the LV micro-CT technique for the analysis of in situ dentitions at different stages of development. For example, there was a marked difference/contrast seen in the density threshold level of the dentine and the enamel for the

teeth from the adults compared with those from the subadults and infant. These variations in density levels were because of the differing stages of dental development and of mineralization of dentitions (Nanci, 2012).

This method can also provide data for an overall impression of general health as well as oral health through the examination of the cranium and the identification of co-morbidities, such as cribra orbitalia (Brickley, 2018; Godde & Hens, 2021; Walker et al., 2009) and caries sicca (Baker et al., 2020). Teeth developing during an extended period of disease or other insult can be affected, and the evidence of such a health insult may be seen as enamel and/or dentine defects (Figures 3–5) (Armelagos et al., 2009; Beaumont et al., 2018; Brickley et al., 2019; Brook et al., 1997; Brook & Smith, 1998; D'Ortenzio, Ribot, et al., 2018; Halcrow & Tayles, 2008; Hillson & Antoine, 2011; Kinaston et al., 2019; Mellanby, 1928, 1934; Nikiforuk & Fraser, 1979).

4.2 | Aim 2 – How findings from the LV micro-CT technique compare with standard methods?

Addressing the second aim, the LV micro-CT was the *only* technique to provide data for the complete analysis of the in situ dentoalveolar complex for the five individuals (Tables 3 and 4). The macroscopic method could not provide all data required for all the categories studied. The radiographic method provided the least amount of information to address the categories (Tables 3 and 4). By combining the macroscopic and the radiographic methods, a range of data could be provided for many but not all of the categories (Table 3).

Differences and similarities were seen in the “level” of scoring of data that was provided from the compared methods. All three techniques produced identical scores for the inventory of the in situ archaeological dentitions, which was to be expected as this category is not open to interpretation. The software (“volren” – Avizo 9) used with the reconstructed LV micro-CT scan data can adjust the density threshold level of the alveolar bone on the 3D images to reveal structures that are denser than the bone tissue, such as the enamel of developing tooth germs (Figure 4). Adjusting the bone density threshold levels and manipulating an image on the computer screen provided valuable additional information on morphology, position, and stage of development of primary and/or permanent teeth within the jaw; this adjustment and visualization of layers are not available on radiographs. The macroscopic method could only provide data for the dental age range category based on evidence of the external eruption of teeth.

The LV micro-CT and radiographic methods identified clinically significant carious lesions having marked demineralization and depth. Early caries with slight demineralization and staining can be scored macroscopically. This may be the reason for the higher caries score in this study with the macroscopic technique (Table 4), but these early reversible changes would have had no influence on the oral or general health of the individual.

The grades for the category of tooth wear were consistently higher on the dental radiographs compared with the other methods. This may have been because of problems associated with superimposition, that is, one structure being superimposed on top of another in the 2D radiographic image. Such distortion of the radiographic image can occur particularly in the cuspal regions of the premolars and molars. To overcome superimposition during the analysis of the Avizo 9 DRR images of the LV micro-CT scans, the clipping tool was used to remove a quadrant of the jaw or individual teeth (Figures 2c, 3, and 4f).

EH defects that were not observed during the macroscopic examination of the teeth of one subadult (SMB 52B) were identified during the 3D image analysis of the LV micro-CT scans. This method also identified a higher total number of EH defects, for all five individuals (Table 4), compared with the macroscopic analysis. The difference in the number of EH defects identified was probably related to the high-resolution images produced by the LV micro-CT system. In addition, an improved level of accurate measurable detail for the location of the EH defects was possible on the 3D image analysis of the LV micro-CT scans compared with the measurements taken during the macroscopic examination. Radiographically, EH is difficult to identify except in the most severe of cases (Figure 5).

For periodontal disease, an improved level of accuracy concerning measuring the distance between the CEJ and the alveolar bone was also provided using the LV micro-CT compared with the macroscopic method (Tables 2 and 4). The LV micro-CT allows for the precise location and size of the defect to be measured or to determine the extent of horizontal alveolar bone loss as evidence of periodontal disease. For example, there was a difference of 1.4 mm between the LV micro-CT measurement and the macroscopic measurement for the same tooth type in individual SMB 73.

4.3 | Illustrative case study: Infant SMB 58

The value of the LV micro-CT method was tested further with the investigation of the dentoalveolar complex in situ in the fragmented skull of infant SMB 58 (approximately 1.5 years of age) (Figures 4 and 6). EH defects were identified macroscopically on several of the erupted primary teeth. To investigate the full extent of this infant's dental and general health, the fragile cranium and mandible were LV micro-CT scanned. This method is ideal for this type of delicate specimen as it offers the least amount of handling of such fragmented remains (Figures 4 and 6).

A change in the bone density threshold levels of the maxilla and mandible on the LV micro-CT scans allowed the developing tooth germs within the alveolar to be analysed. Evidence of extensive EH defects was seen on the developing permanent teeth, the semi-erupted and erupted primary teeth (Figure 4). Examination of the dentine of the erupted and developing dentitions of this infant showed areas of IGD (Figure 6). These enamel secretion and dentine mineralization defects indicate that the ameloblast and the odontoblast (Hillson, 1996; Nanci, 2012) were affected by health insults during the

development of the primary and permanent dentitions and reflect the general health status of infant SMB 58. An approximation of the timing of the health insults, during the development of the dentition (AlQahtani, 2012; AlQahtani et al., 2010), can be made by examining the location of the defects in relation to the CEJ. Health insults, such as a chronic systemic illness in the pregnant mother, can affect the primary and permanent dentitions of a baby in utero. Postnatally, the temporary immunity passed on to the newborn from its mother via the placenta and through breastfeeding (Jennewein et al., 2017) decreases, and the infant's immature immune system can struggle to overcome health issues. The location of the EH defects seen on the primary and developing permanent dentition of SMB 58 suggests that they could have suffered a health insult around the time of birth, and further illness affecting the developing teeth of this infant in the first year of life (AlQahtani et al., 2010; Nanci, 2012). The additional information gained from the LV micro-CT scan of the dentoalveolar complex of SMB 58 adds to the data from the macroscopic and radiographic methods (Figure 5) and illustrates the importance of this imaging technique.

4.4 | Advantages and limitations of the large volume micro-CT scanning method

The LV micro-CT scanning system is a valuable method that has shown it can be used as a single technique for the investigation of the dentoalveolar complex in situ in human archaeological skulls. Moreover, this micro-CT scanning system is considerably more time efficient for the amount of data received than by combining the macroscopic and radiographic methods.

Digital images (2D and 3D) created from LV micro-CT scans are permanent records that could be used to preserve rare and/or delicate archaeological human skull samples from individuals of different age groups as well as for data sharing for international collaboration, and/or for repeat scoring for reproducibility studies. Alternatively, micro-CT scan data sets can be converted to STL files for 3D printing. Ethical implications of digitalizing and/or replicating human remains must always be considered (Hirst et al., 2018).

4.5 | Alternative 3D image analysis techniques

An alternative CT technique that was not utilized for this investigation but could also be used for the study of the dentoalveolar complex in situ in human skull samples was the CBCT scanner. As previously mentioned, there is a difference in the size of the scan slice produced by the two techniques (Orhan, 2020; Orhan & Büyüksungur, 2019; Pour et al., 2016). However, depending on the type of anatomical or pathology structure to be studied, the CBCT scanner may be more readily available and a cheaper alternative to the LV micro-CT scanner (Lamira et al., 2022; Lozano et al., 2022). The 3D digital microscope (3D DM) could also provide high-quality images of dental defects on the external surfaces of the teeth. This equipment is suitable for teeth

in situ in "small maxilla and mandible fragments or isolated teeth" (Lozano et al., 2022:3) but not an entire in situ dentoalveolar complex.

4.6 | Limitations of this study

The sample size for this study was dictated by the cost of the LV micro-CT technique. While at present the LV micro-CT is used for small numbers of rare samples, the cost is likely to reduce as the method becomes more widely applied. Statistical analysis (Gwet's AC and AC2) was affected by the sample size (Tables S3 and S4), with many results having a confidence interval of 1.00, which indicates a perfect agreement by the operators (raters).

5 | CONCLUSION

The LV micro-CT scanning technique was the only method to provide data for all the categories studied. This micro-CT scanning system provides accurate, detailed measurements of external and internal structures of the dentoalveolar complex in situ within archaeological human skull specimens. In this study, the LV micro-CT technique provided data that could not be obtained using macroscopic or radiographic methods and demonstrates that LV micro-CT scanning is an advance from standard non-invasive methods. This valuable technique allows fragile and rare archaeological human skull specimens to be examined, as the study of infant SMB 58 illustrated. The data that support the findings are available from the corresponding author upon reasonable request.

ACKNOWLEDGMENTS

Fr. William Deng, of St Mary's Anglican Church, provided access to the St Mary's skeletal sample and the parish records. Funding for this research is from the University of Adelaide, Adelaide Dental School Research grant. The facilities and the scientific and technical assistance of the Australian Microscopy and Microanalysis Research Facility at Adelaide Microscopy, University of Adelaide are acknowledged, in particular, Dr. Agatha Labrinidis Associate Professor Egon Perilli from the Medical Device Research Institute, College of Science and Engineering, Flinders University, shared his expertise regarding the Large Volume micro-CT system. Flinders Microscopy and Microanalysis (FMMA) provided access to the new Nikon XT H 225 ST micro-CT scanning system. The Australian Research Council (LE180100136) provided a funding contribution for the procurement of the Large Volume micro-CT system. Dr Derek Lerche from the Adelaide Dental School provided assistance with the dental radiographs. Dr John Wetherell, Claudia Barrientos, and Ella Kelty, who undertook reproducibility scoring.

CONFLICT OF INTEREST

The authors declare that they have no known competing financial interests or personal relationships that could have appeared to influence the work reported in this paper.

DATA AVAILABILITY STATEMENT

The data that support the findings of this study are available from the corresponding author upon reasonable request.

ORCID

Angela Gurr  <https://orcid.org/0000-0002-9097-9130>

Denice Higgins  <https://orcid.org/0000-0001-7780-243X>

REFERENCES

- AlQahtani, S. (2012). *The London Atlas: Developing an atlas of tooth development and testing its quality and performance measures*. ProQuest Dissertations Publishing.
- AlQahtani, S. J., Hector, M. P., & Liversidge, H. M. (2010). Brief communication: The London Atlas of human tooth development and eruption. *American Journal of Physical Anthropology*, 142, 481–490. <https://doi.org/10.1002/ajpa.21258>
- Alsop, K., Norman, D. G., Baier, W., Colclough, J., & Williams, M. A. (2022). Advantages of micro-CT in the case of a complex dismemberment. *Journal of Forensic Sciences*, 67, 1258–1266. <https://doi.org/10.1111/1556-4029.15007>
- Anderson, P. J., Yong, R., Surman, T. L., Rajion, Z. A., & Ranjitkar, S. (2014). Application of three-dimensional computed tomography in craniofacial clinical practice and research. *Australian Dental Journal*, 59(s1), 174–185. <https://doi.org/10.1111/adj.12154>
- Angel, J. L. (1966). Porotic hyperostosis, anemias, malaras, and marshes in the prehistoric eastern Mediterranean. *Science (New York, N.Y.)*, 153, 760–763. <https://doi.org/10.1126/science.153.3737.760>
- Anson, T. J. (2004). The bioarchaeology of the St. Mary's free ground burials: Reconstruction of colonial South Australian lifeways, Thesis (Ph.D.). University of Adelaide, Dept. of Anatomical Sciences, 2004.
- Appleby, J. D., Ruddy, G. N., Hainsworth, S. V., Woosnam-Savage, R. C., Morgan, B., Brough, A., Earp, R. W., Robinson, C., King, T. E., Morris, M., & Buckley, R. (2015). Perimortem trauma in King Richard III: A skeletal analysis. *The Lancet (British Edition)*, 385(9964), 253–259. [https://doi.org/10.1016/S0140-6736\(14\)60804-7](https://doi.org/10.1016/S0140-6736(14)60804-7)
- Araújo, M. G., Silva, C. O., Misawa, M., & Sukekava, F. (2015). Alveolar socket healing: What can we learn? *Periodontology*, 2000(68), 122–134.
- Armstrong, G. J., Goodman, A. H., Harper, K. N., & Blakey, M. L. (2009). Enamel hypoplasia and early mortality: Bioarchaeological support for the Barker hypothesis. *Evolutionary Anthropology: Issues, News, and Reviews*, 18, 261–271. <https://doi.org/10.1002/evan.20239>
- Baker, B. J., Crane-Kramer, G., Dee, M. W., Gregoricka, L. A., Henneberg, M., Lee, C., Lukehart, S. A., Mabey, D. C., Roberts, C. A., Stodder, A. L. W., Stone, A. C., & Winingear, S. (2020). Advancing the understanding of treponemal disease in the past and present. *American Journal of Physical Anthropology*, 171, 5–41. <https://doi.org/10.1002/ajpa.23988>
- Beaumont, J., Atkins, E. C., Buckberry, J., Haydock, H., Horne, P., Howcroft, R., Mackenzie, K., & Montgomery, J. (2018). Comparing apples and oranges: Why infant bone collagen may not reflect dietary intake in the same way as dentine collagen. *American Journal of Physical Anthropology*, 167, 524–540. <https://doi.org/10.1002/ajpa.23682>
- Beetge, M. M., Todorovic, V. S., Oettlé, A., Hoffman, J., & Zyl, A. W. V. (2018). A micro-CT study of the greater palatine foramen in human skulls. *Journal of Oral Science*, 60, 51–56. <https://doi.org/10.2334/josnusd.16-0783>
- Braun, S., Ridel, A. F., L'Abbé, E. N., Theye, C. E. G., & Oettlé, A. C. (2022). Repeatability of a morphoscopic sex estimation technique for the mental eminence on micro-focus X-ray computed tomography models. *Forensic Imaging (Online)*, 28, 200500. <https://doi.org/10.1016/j.fri.2022.200500>
- Brickley, M. (2018). Cribra orbitalia and porotic hyperostosis: A biological approach to diagnosis. *American Journal of Physical Anthropology*, 167, 896–902. <https://doi.org/10.1002/ajpa.23701>
- Brickley, M. B., Kahlon, B., & D'Ortenzio, L. (2019). Using teeth as tools: Investigating the mother-infant dyad and developmental origins of health and disease hypothesis using vitamin D deficiency. *American Journal of Physical Anthropology*, 171, 342–353. <https://doi.org/10.1002/ajpa.23947>
- Brook, A., 2014. Research contributions to paediatric dentistry in the areas of dental development, orofacial pathology, prevention, education and patient management.
- Brook, A., Fearn, J., & Smith, J. (1997). Environmental causes of enamel defects. *Dental Enamel*, 205, 212–225. <https://doi.org/10.1002/9780470515303.ch15>
- Brook, A. H. (2009). Multilevel complex interactions between genetic, epigenetic and environmental factors in the aetiology of anomalies of dental development. *Archives of Oral Biology*, 54, S3–S17. <https://doi.org/10.1016/j.archoralbio.2009.09.005>
- Brook, A. H., Brook O'Donnell, M., Hone, A., Hart, E., Hughes, T. E., Smith, R. N., & Townsend, G. C. (2014). General and craniofacial development are complex adaptive processes influenced by diversity. *Australian Dental Journal*, 59, 13–22. <https://doi.org/10.1111/adj.12158>
- Brook, A. H., Elcock, C., Hallonsten, A. L., Poulsen, S., Andreasen, J., Koch, G., Yeung, C. A., & Dosanjh, T. (2001). The development of a new index to measure enamel defects. In A. H. Brook (Ed.), *Dental morphology* (pp. 59–66). Sheffield Academic Press.
- Brook, A. H., Koh, K. S. B., & Toh, V. K. L. (2016). Influences in a biologically complex adaptive system: Environmental stress affects dental development in a group of Romano-Britons. *International Journal of Design and Nature and Ecodynamics*, 11, 33–40. <https://doi.org/10.2495/DNE-V11-N1-33-40>
- Brook, A. H., & O'Donnell, B. (2022). Complexity, networking and many model thinking enhance understanding of patterning, variation and interactions of human teeth and dental arches. In D. Chen & P. Ahlberg (Eds.), *Section 4 in odontodes: The development and evolutionary building blocks of dentitions*. CRC Press.
- Brook, A. H., & Smith, J. M. (1998). The aetiology of developmental defects of enamel: A prevalence and family study in East London, U.K. *Connective Tissue Research*, 39, 151–156. <https://doi.org/10.3109/03008209809023921>
- Brook, A. H., & Smith, J. M. (2006). Hypoplastic enamel defects and environmental stress in a homogeneous Romano-British population. *European Journal of Oral Sciences*, 114, 370–374. <https://doi.org/10.1111/j.1600-0722.2006.00306.x>
- Clement, A. M., Cloutier, R., Lu, J., Perilli, E., Maksimenko, A., & Long, J. (2021). A fresh look at Cladarosymblesma narrienense, a tetrapodomorph fish (Sarcopterygii: Megalichthyidae) from the carboniferous of Australia, illuminated via X-ray tomography. *PeerJ (San Francisco, CA)*, 9, e12597.
- Colombo, A., Ortenzio, L., Bertrand, B., Coqueugnot, H., Knüsel, C. J., Kahlon, B., & Brickley, M. (2019). Micro-computed tomography of teeth as an alternative way to detect and analyse vitamin D deficiency. *Journal of Archaeological Science: Reports*, 23, 390–395.
- D'Ortenzio, L., Kahlon, B., Peacock, T., Salahuddin, H., & Brickley, M. (2018). The rachitic tooth: Refining the use of interglobular dentine in diagnosing vitamin D deficiency. *International Journal of Paleopathology*, 22, 101–108. <https://doi.org/10.1016/j.ijpp.2018.07.001>
- D'Ortenzio, L., Ribot, I., Kahlon, B., Bertrand, B., Bocaage, E., Raguin, E., Schattmann, A., & Brickley, M. (2018). The rachitic tooth: The use of radiographs as a screening technique. *International Journal of Paleopathology*, 23, 32–42. <https://doi.org/10.1016/j.ijpp.2017.10.001>
- du Plessis, A., Broeckhoven, C., Guelpa, A., & le Roux, S. G. (2017). Laboratory x-ray micro-computed tomography: A user guideline for biological samples. *Gigascience*, 6, 1–11. <https://doi.org/10.1093/gigascience/gix027>
- Efremov, J. A. (1940). Taphonomy: New branch of paleontology. *American Geologist*, 74, 81–93.

- Elcock, C., Lath, D. L., Luty, J. D., Gallagher, M. G., Abdellatif, A., Backman, B., & Brook, A. (2006). The new enamel defects index: Testing and expansion. *European Journal of Oral Sciences*, 114, 35–38. <https://doi.org/10.1111/j.1600-0722.2006.00294.x>
- FDI World dental Federation. (2022). *FDI two-digit notation*. FDI World Dental Federation.
- Fraberger, S., Dockner, M., Winter, E., Pretterklieber, M., Weber, G. W., Teschler-Nicola, M., & Pietschmann, P. (2021). Micro-CT evaluation of historical human skulls presenting signs of syphilitic infection. *Wiener Klinische Wochenschrift*, 133, 602–609. <https://doi.org/10.1007/s00508-021-01832-z>
- Garot, E., Couture-Veschambre, C., Manton, D., Beauval, C., & Rouas, P. (2017). Analytical evidence of enamel hypomineralisation on permanent and primary molars amongst past populations. *Scientific Reports*, 7, 1712–1710. <https://doi.org/10.1038/s41598-017-01745-w>
- Garot, E., Couture-Veschambre, C., Manton, D., Bekvalac, J., & Rouas, P. (2019). Differential diagnoses of enamel hypomineralisation in an archaeological context: A postmedieval skeletal collection reassessment. *International Journal of Osteoarchaeology*, 29, 747–775. <https://doi.org/10.1002/oa.2785>
- Godde, K., & Hens, S. M. (2021). An epidemiological approach to the analysis of cribra orbitalia as an indicator of health status and mortality in medieval and post-medieval London under a model of parasitic infection. *American Journal of Physical Anthropology*, 174, 631–645. <https://doi.org/10.1002/ajpa.24244>
- Grace, T. M., O'Rourke, D., Robertson, T., Perilli, E., Callary, S., Taylor, M., Atkins, G. J., Solomon, L. B., & Thewlis, D. (2022). A semiautomated method to quantitatively assess osteolytic lesion volume and bone mineral density within acetabular regions of interest from CT. *Journal of Orthopaedic Research*, 40, 396–408. <https://doi.org/10.1002/jor.25051>
- Gurr, A., Brook, A. H., Kumaratilake, J., Anson, T., Pate, F. D., & Henneberg, M. (2022). Was it worth migrating to the new British industrial colony of South Australia? Evidence from skeletal pathologies and historic records of a sample of 19th-century settlers. *International Journal of Paleopathology*, 37, 41–52. <https://doi.org/10.1016/j.ijpp.2022.04.002>
- Gurr, A., Kumaratilake, J., Brook, A. H., Ioannou, S., Pate, F. D., & Henneberg, M. (2022). Health effects of European colonization: An investigation of skeletal remains from 19th to early 20th century migrant settlers in South Australia. *PLoS ONE*, 17, e0265878–e0265878. <https://doi.org/10.1371/journal.pone.0265878>
- Halcrow, S. E., & Tayles, N. (2008). Stress near the start of life? Localised enamel hypoplasia of the primary canine in late prehistoric mainland Southeast Asia. *Journal of Archaeological Science*, 35, 2215–2222. <https://doi.org/10.1016/j.jas.2008.02.002>
- Heuck Henriksson, C., Andersson, M. E.-M., & Møystad, A. (2019). Hypodontia and retention of third molars in Norwegian medieval skeletons: Dental radiography in osteoarchaeology. *Acta Odontologica Scandinavica*, 77, 310–314. <https://doi.org/10.1080/00016357.2018.1549749>
- Hillson, S. (1996). *Dental anthropology*. Cambridge University Press. 10.1017/CBO9781139170697
- Hillson, S., & Antoine, D. (2011). The mechanisms that produce the defects of enamel hypoplasia. *American Journal of Physical Anthropology*, 144, 163–163.
- Hirst, C. S., White, S., & Smith, S. E. (2018). Standardisation in 3D geometric morphometrics: Ethics, Ownership, and Methods. *Archaeologies*, 14, 272–298. <https://doi.org/10.1007/s11759-018-9349-7>
- Hutchinson, E. F., Florentino, G., Hoffman, J., & Kramer, B. (2016). Micro-CT assessment of changes in the morphology and position of the immature mandibular canal during early growth. *Surgical and Radiologic Anatomy (English Ed.)*, 39, 185–194. <https://doi.org/10.1007/s00276-016-1694-x>
- International Caries Classification and Management System. (2020). Contents: ICCMS-Usage: Research. <https://iccms-web/content/iccms-usage/research>.
- International Organisation for Standardization, American National Standard, American Dental Association. (2010). Specification No. 3950. Designation System for Teeth and Areas of the Oral Cavity, American Dental Association, Switzerland.
- Jennewein, M. F., Abu-Raya, B., Jiang, Y., Alter, G., & Marchant, A. (2017). Transfer of maternal immunity and programming of the newborn immune system. *Seminars in Immunopathology*, 39, 605–613. <https://doi.org/10.1007/s00281-017-0653-x>
- Kerekes-Mathe, B., Brook, A., Martha, K., Szekely, M., & Smith, R. N. (2015). Mild hypodontia is associated with smaller tooth dimensions and cusp numbers than in controls. *Archives of Oral Biology*, 60, 1442–1449. <https://doi.org/10.1016/j.archoralbio.2015.06.005>
- Kinaston, R., Willis, A., Miszkiewicz, J. J., Tromp, M., & Oxenham, M. F. (2019). The dentition: Development, disturbances, disease, diet, and chemistry. In J. E. Buikstra (Ed.), *Ortner's identification of paleopathological conditions in human skeletal remains* (Third ed.). Academic Press. <https://doi.org/10.1016/B978-0-12-809738-0.00021-1>
- Kramer, B., Molema, K., & Hutchinson, E. F. (2019). An osteological assessment of cyclopia by micro-CT scanning. *Surgical and Radiologic Anatomy (English Ed.)*, 41, 1053–1063. <https://doi.org/10.1007/s00276-019-02284-x>
- Kusins, J., Knowles, N., Ryan, M., Dall'Ara, E., & Ferreira, L. (2019). Performance of QCT-derived scapula finite element models in predicting local displacements using digital volume correlation. *Journal of the Mechanical Behavior of Biomedical Materials*, 97, 339–345. <https://doi.org/10.1016/j.jmbbm.2019.05.021>
- Lacy, S. A., Wu, X. J., Jin, C. Z., Qin, D. G., Cai, Y. J., & Trinkaus, E. (2012). Dentoalveolar paleopathology of the early modern humans from Zhirendong, South China. *International Journal of Paleopathology*, 2, 10–18. <https://doi.org/10.1016/j.ijpp.2012.06.003>
- Lamira, A., Mazzi-Chaves, J. F., Nicolielo, L. F. P., Leoni, G. B., Silva-Sousa, A. C., Silva-Sousa, Y. T. C., Pauwels, R., Buls, N., Jacobs, R., & Sousa-Neto, M. D. (2022). CBCT-based assessment of root canal treatment using micro-CT reference images. *Imaging Science in Dentistry*, 52, 245–258. <https://doi.org/10.5624/isd.20220019>
- Litzlbauer, H. D., Neuhaeuser, C., Moell, A., Greschus, S., Breithecker, A., Franke, F. E., Kummer, W., & Rau, W. S. (2006). Three-dimensional imaging and morphometric analysis of alveolar tissue from microfocal X-ray-computed tomography. *American Journal of Physiology - Lung Cellular and Molecular Physiology*, 291, 535–545.
- Lozano, M., Gamarra, B., Hernando, R., & Ceperuelo, D. (2022). Microscopic and virtual approaches to oral pathology: A case study from El Mirador Cave (Sierra de Atapuerca, Spain). *Annals of Anatomy*, 239, 151827–151827. <https://doi.org/10.1016/j.aanat.2021.151827>
- Main, M., Tan, J., Yong, R., Williams, R., Labrinidis, A., Anderson, P. J., & Ranjitkar, S. (2021). Craniofacial phenomics: Three-dimensional assessment of the size and shape of cranial and dentofacial structures. In S. Dworkin (Ed.), *Craniofacial development*. Methods Molecular Biology. Humana. https://doi.org/10.1007/978-1-0716-1847-9_9
- Manzi, G., Salvadei, L., Vienna, A., & Passarello, P. (1999). Discontinuity of life conditions at the transition from the Roman imperial age to the early middle ages: Example from Central Italy evaluated by pathological dento-alveolar lesions. *American Journal of Human Biology*, 11, 327–341. [https://doi.org/10.1002/\(SICI\)1520-6300\(1999\)11:3<327::AID-AJHB5>3.0.CO;2-M](https://doi.org/10.1002/(SICI)1520-6300(1999)11:3<327::AID-AJHB5>3.0.CO;2-M)
- Mellanby, M. (1928). Defective structure of teeth. *The British Medical Journal*, 1, 410–410. <https://doi.org/10.1136/bmj.1.3505.410>
- Mellanby, M. (1934). Diet and the teeth: An experimental study. Part III. The effect of diet on dental structure and disease in man. *Journal of the American Medical Association*, 102, 1523–1523. <https://doi.org/10.1001/jama.1934.02750180075026>
- Minnema, J., van Eijnatten, M., Kouw, W., Diblen, F., Mendrik, A., & Wolff, J. (2018). CT image segmentation of bone for medical additive manufacturing using a convolutional neural network. *Computers in*

- Biology and Medicine*, 103, 130–139. <https://doi.org/10.1016/j.combiomed.2018.10.012>
- Molnar, S. (1971). Human tooth wear, tooth function and cultural variability. *American Journal of Physical Anthropology*, 34, 175–189. <https://doi.org/10.1002/ajpa.1330340204>
- Nanci, A. (2012). *Ten Cate's oral histology: Development, structure, and function*. Elsevier, Saint Louis.
- Nikiforuk, G., & Fraser, D. (1979). Etiology of enamel hypoplasia and Interlobular dentin: The roles of hypocalcemia and hypophosphatemia. *Metabolic Bone Disease and Related Research*, 2, 17–23. [https://doi.org/10.1016/0221-8747\(79\)90014-6](https://doi.org/10.1016/0221-8747(79)90014-6)
- Nikolova, S., Toneva, D., Georgiev, I., & Lazarov, N. (2019). Sagittal suture maturation: Morphological reorganization, relation to aging, and reliability as an age-at-death indicator. *American Journal of Physical Anthropology*, 169, 78–92. <https://doi.org/10.1002/ajpa.23810>
- Nikon Metrology. (2021). Products: X-ray and CT Technology: X-ray and CT systems: 225kV and 320kV CT inspection and metrology.
- Ogden, A. R., Pinhasi, R., & White, W. J. (2007). Gross enamel hypoplasia in molars from subadults in a 16th–18th century London graveyard. *American Journal of Physical Anthropology*, 133, 957–966. <https://doi.org/10.1002/ajpa.20608>
- Orhan, K. (2020). *Micro-computed tomography (micro-CT) in medicine and engineering* (1st 2020 ed.) (10.1007/978-3-030-16641-0). Springer International Publishing.
- Orhan, K., & Büyüksungur, A. (2019). *Fundamentals of micro-CT imaging* (pp. 27–33). Springer International Publishing. https://doi.org/10.1007/978-3-030-16641-0_3
- Patel, D., Sassani, S., Farella, M., Ranjitkar, S., Yong, R., Swindells, S., & Brook, A. (2018). Variations in dental arch morphology are outcomes of the complex adaptive system associated with the developmental variation of hypodontia. *International Journal of Design & Nature and Ecodynamics*, 13, 107–113. <https://doi.org/10.2495/DNE-V13-N1-107-113>
- Perilli, E., Parkinson, I. H., & Reynolds, K. J. (2012). Micro-CT examination of human bone: From biopsies towards the entire organ. *Annali dell'Istituto Superiore di Sanità*, 48, 75–82. https://doi.org/10.4415/ANN_12_01_13
- Perschbacher, S. (2014). Periodontal Diseases. In S. C. White & M. J. Pharoah (Eds.). *Oral radiology: Principles and interpretations* (pp. 299–313). Elsevier. <https://doi.org/10.1016/B978-0-323-09633-1.00019-5>
- Pitts, N. B., & Ekstrand, K. R. (2013). International caries detection and assessment system (ICDAS) and its international caries classification and management system (ICCMS)—Methods for staging of the caries process and enabling dentists to manage caries. *Community Dentistry and Oral Epidemiology*, 41, e41–e52. <https://doi.org/10.1111/cdoe.12025>
- Planmeca. (2022). Intraoral X-ray unit, Planmeca OY. KaVo Dental GmbH, nd. KaVo Imaging Solutions: KaVo Pan eXam Plus., KaVo Dental GmbH.
- Pour, D., Arzi, B., & Shamshiri, A. (2016). Assessment of slice thickness effect on visibility of inferior alveolar canal in cone beam computed tomography images. *Dental Research Journal*, 13, 527–531. <https://doi.org/10.4103/1735-3327.197041>
- Riga, A., Begni, C., Sala, S., Erriu, S., Gori, S., Moggi-Cecchi, J., Mori, T., & Dori, I. (2021). Is root exposure a good marker of periodontal disease? *Bulletin of the International Association of Paleodontology*, 15, 21–30.
- Rutty, G. N., Brough, A., Biggs, M. J. P., Robinson, C., Lawes, S. D. A., & Hainsworth, S. V. (2012). The role of micro-computed tomography in forensic investigations. *Forensic Science International*, 225, 60–66.
- Smilg, J. S. (2017). Finding fossils in Malapa breccia—Medical CT: Scanning or micro-CT scanning? *South African Journal of Science*, 113(11–12), 1–6. <https://doi.org/10.17159/sajs.2017/20170057>
- Smit, S., Hutchinson, E. F., & Kramer, B. (2020). A morphometric analysis of the immature human infraorbital canal. *Surgical and Radiologic Anatomy (English Ed.)*, 43, 201–210. <https://doi.org/10.1007/s00276-020-02563-y>
- Stan, A. T., Cirligeriu, L., Idrasi, L., Negruțiu, M. L., Sinescu, C., Pop, D. M., Hajaj, T., Talpoș, Ș., & Romînu, M. (2019). Marginal and internal adaptation evaluation of dental composites using micro-CT. *Advances in Materials Science and Engineering*, 2019, 1–6. <https://doi.org/10.1155/2019/5010319>
- Tan, J., Labrinidis, A., Williams, R., Main, M., Anderson, P. J., & Ranjitkar, S. (2022). Micro-CT-based bone microarchitecture analysis of the murine skull. In S. Dworkin (Ed.). *Craniofacial development*. Methods of Molecular Biology. Humana. https://doi.org/10.1007/978-1-0716-1847-9_10
- ThermoFisher Scientific. (2019). 3D Visualization & Analysis Software: Amiro-Avizo.
- Theye, C. E. G., Hattingh, A., Cracknell, T. J., Oetllé, A. C., Steyn, M., & Vandeweghe, S. (2018). Dento-alveolar measurements and histomorphometric parameters of maxillary and mandibular first molars, using micro-CT. *Clinical Implant Dentistry and Related Research*, 20, 550–561. <https://doi.org/10.1111/cid.12616>
- Trinkaus, E., Lacy, S. A., Thibeault, A., & Villotte, S. (2021). Disentangling Cro-Magnon: The dental and alveolar remains. *Journal of Archaeological Science: Reports*, 37, 102911. <https://doi.org/10.1016/j.jasrep.2021.102911>
- Veselka, B., Brickley, M. B., D'Ortenzio, L., Kahlon, B., Hoogland, M. L. P., & Waters-Rist, A. L. (2019). Micro-CT assessment of dental mineralization defects indicative of vitamin D deficiency in two 17th–19th century Dutch communities. *American Journal of Physical Anthropology*, 169, 1–10. <https://doi.org/10.1002/ajpa.23819>
- Walker, P. L., Bathurst, R. R., Richman, R., Gjerdrum, T., & Andrushko, V. A. (2009). The causes of porotic hyperostosis and cribra orbitalia: A reappraisal of the iron-deficiency-anemia hypothesis. *American Journal of Physical Anthropology*, 139, 109–125. <https://doi.org/10.1002/ajpa.21031>
- Wearne, L. S., Rapagna, S., Taylor, M., & Perilli, E. (2022). Micro-CT scan optimisation for mechanical loading of tibia with titanium tibial tray: A digital volume correlation zero strain error analysis. *Journal of the Mechanical Behavior of Biomedical Materials*, 134, 105336–105336. <https://doi.org/10.1016/j.jmbbm.2022.105336>
- Welsh, H., Nelson, A. J., van der Merwe, A. E., de Boer, H. H., & Brickley, M. B. (2020). An investigation of micro-CT analysis of bone as a new diagnostic method for paleopathological cases of osteomalacia. *International Journal of Paleopathology*, 31, 23–33. <https://doi.org/10.1016/j.ijpp.2020.08.004>
- Willmann, C., Mata, X., Hanghoej, K., Tonasso, L., Tisseyre, L., Jeziorski, C., Cabot, E., Chevet, P., Crubézy, E., Orlando, L., Esclassan, R., & Thèves, C. (2018). Oral health status in historic population: Macroscopic and metagenomic evidence. *PLoS ONE*, 13, e0196482. <https://doi.org/10.1371/journal.pone.0196482>
- Winter, G. B., & Brook, A. H. (1989). Injuries (traumatic). In A. H. R. Rowe, A. G. Alexander, & R. B. Johns (Eds.). *A comprehensive guide to clinical dentistry* (pp. 104–111). Class Publishing, Somerset, UK.

SUPPORTING INFORMATION

Additional supporting information can be found online in the Supporting Information section at the end of this article.

How to cite this article: Gurr, A., Higgins, D., Henneberg, M., Kumaratilake, J., O'Donnell, M. B., McKinnon, M., Hall, K. A., & Brook, A. H. (2023). Investigating the dentoalveolar complex in archaeological human skull specimens: Additional findings with large volume micro-CT compared to standard methods. *International Journal of Osteoarchaeology*, 33(2), 235–250. <https://doi.org/10.1002/oa.3204>